

# Matrix infrared spectroscopic studies of the photo-dissociation at 266 nm of ClNO<sub>2</sub> and of ClONO

J.M. Coanga<sup>a</sup>, L. Schriver-Mazzuoli<sup>a,b,\*</sup>, A. Schriver<sup>a</sup>, P.R. Dahoo<sup>c</sup>

<sup>a</sup> Laboratoire de Physique Moléculaire et Applications, Laboratoire propre du CNRS, Université Pierre et Marie Curie, Tour 13, case 76, 4 place Jussieu, 75252 Paris Cedex 05, France

<sup>b</sup> Laboratoire d'Etude des Nuisances Atmosphériques et de leurs Effets, Université Paris-Nord Campus de Bobigny, IUP Ville et Santé, Rue de la Convention, Bobigny 93017, France

<sup>c</sup> Laboratoire de Magnétisme et d'Optique de Versailles, Université de Versailles St Quentin en Yvelines, 45 Avenue des Etats Unis, 78035 Versailles Cedex, France

Received 4 September 2001; in final form 14 November 2001

## Abstract

Detailed infrared spectroscopic studies of the photo-dissociation at 266 nm of ClNO<sub>2</sub> trapped in argon matrices with subsequent experiments conducted with a xenon lamp at  $\lambda > 360$  nm are reported. Formation of *cis* and *trans* ClONO in equilibrium with ClNO<sub>2</sub> is observed after irradiation at 266 nm. At  $\lambda > 360$  nm the transformation of *trans* ClONO into *cis* ClONO occurs. On prolonged photolysis at 266 nm, ClONO dissociates into ClON and O(<sup>1</sup>D) atom and into ClO + NO as evidenced in reactive matrices (solid oxygen and nitrogen). © 2002 Published by Elsevier Science B.V.

## 1. Introduction

Over the past two decades, it has become evident that nitryl chloride (ClNO<sub>2</sub>) and its isomers (ClONO *cis* and *trans*) play an important role in the chemistry of both the troposphere and stratosphere. In the troposphere, production of ClNO<sub>2</sub> occurs from the reaction of gaseous N<sub>2</sub>O<sub>5</sub> with NaCl salt aerosol [1,2]. In the stratosphere, fast reaction of N<sub>2</sub>O<sub>5</sub> with HCl dissolved in ice leads to HNO<sub>3</sub> (solid) and ClNO<sub>2</sub> [3]. The *cis* isomer ClONO has been observed in the gas phase by

reactions between atomic chlorine and NO<sub>2</sub> [4] or between Cl<sub>2</sub>O and ClNO [5]. It isomerized slowly into ClNO<sub>2</sub>.

While in the atmosphere ClNO<sub>2</sub> is assumed to be rapidly photolysed after sunrise (in less than 1 h) yielding to Cl atoms and NO<sub>2</sub>, in condensed phase, photo-dissociation of ClNO<sub>2</sub> can be different due to the cage effect. Tevault and Smardzewski [6] reported an apparent conversion from ClONO *trans* (produced in argon matrix from Cl and NO<sub>2</sub>) to ClNO<sub>2</sub>. In their study of photo-isomerization of nitryl bromide to *trans* BrONO in argon matrix, Scheffer et al. [7] reported that ClNO<sub>2</sub> was converted by UV light into a mixture of *cis* and *trans* ClONO. In the present work, we report a detailed infrared spectroscopic study of the photo-dissociation at 266 nm of

\* Corresponding author. Fax: +1-4427-7033.

E-mail address: schriver@ccr.jussieu.fr (L. Schriver-Mazzuoli).

$\text{ClNO}_2$  trapped in argon, oxygen and nitrogen matrices. Subsequent experiments in argon matrix have also been conducted with a xenon lamp at  $\lambda > 360$  nm.

## 2. Experimental

Normal  $\text{ClNO}_2$  was synthesized by the reaction of an excess of ozone with nitrosyl chloride ( $\text{ClNO}$ ) at room temperature [8]. Ozone was prepared by silent electrical discharge through oxygen in a closed system cooled with liquid nitrogen using  $\text{O}_2$  N 45 pure from Air Liquide.  $\text{ClNO}$  from Merck Schuchardt was condensed at 77 K and subjected to several freeze–pump–thaw cycles before being mixed with ozone. After the reaction of  $\text{O}_3$  with  $\text{ClNO}$ , residual oxygen was removed by the pumping on the  $-180$  °C condensate followed by purification of  $\text{ClNO}_2$  by trap to trap distillation at  $-70$  °C.

Matrix samples  $\text{M}/\text{ClNO}_2$  of molar ratio of 5000 were prepared using standard manometric procedures. Ar,  $\text{N}_2$  and  $\text{O}_2$  were obtained commercially with a purity greater than 99.9995% and used without purification. The studies were performed using a closed cycle helium refrigerator Air Product Displex 202 A with a rotating base which allowed one to place the sample either in front of the spectrometer beam or in a perpendicular direction in front of the photolysis sources through  $\text{KBr}$  or  $\text{CaF}_2$  windows, respectively. Matrix gases were deposited onto a golden mirror held at 20 K (Ar,  $\text{O}_2$ ) or 17 K ( $\text{N}_2$ ) with a deposition rate of about  $10 \text{ m mol h}^{-1}$ . Reflected infrared spectra were recorded at 11 K by a Bruker IRTF 113 v over the range  $4000\text{--}500 \text{ cm}^{-1}$  at a resolution of  $0.5 \text{ cm}^{-1}$ .

Two different photolysis sources were employed: a Nd-Yag laser from Quantel (YG 781-20C) at 266 nm and operating at 20 Hz and a xenon lamp, Cunow XC 150 S 150 W used with a cut-off 360 nm filter (Schott WG 360).

## 3. Vibrational spectrum of $\text{ClNO}_2$

The IR spectrum of nitrogen 14 and nitrogen 15 isotopic species of nitryl chloride has been

examined in the vapour state and solid state 30 years ago [9]. More recently the  $\nu_1$  ( $\nu_{\text{NO}}^{\text{S}}$  symmetric stretching mode) and  $2\nu_6$  (out of plane wagging harmonic mode) bands which are in Fermi resonance have been studied by high resolution using Fourier transform spectroscopy. The rotational constants in the  $\nu_1 = 1$  and  $\nu_6 = 2$  vibrational states of  $^{35}\text{ClNO}_2$  were determined by least square calculations [10]. In matrices, relatively little is known about the spectrum of  $\text{ClNO}_2$ . Some bands have been identified by Tevault and Smardzewski [6] after the reaction of Cl with  $\text{NO}_2$ . Preliminary to photolysis experiments, we have recorded the spectrum of  $\text{ClNO}_2$  highly diluted in argon, nitrogen and oxygen matrices ( $\text{ClNO}_2/\text{M} = 1/5000$ ) between  $4000$  and  $500 \text{ cm}^{-1}$ . Fig. 1 shows the key regions in argon matrices, obtained after deposition and after annealing. Frequencies and relative intensities of the observed bands are summarized in Table 1 and compared with those measured in nitrogen and oxygen matrices and in the gas phase.

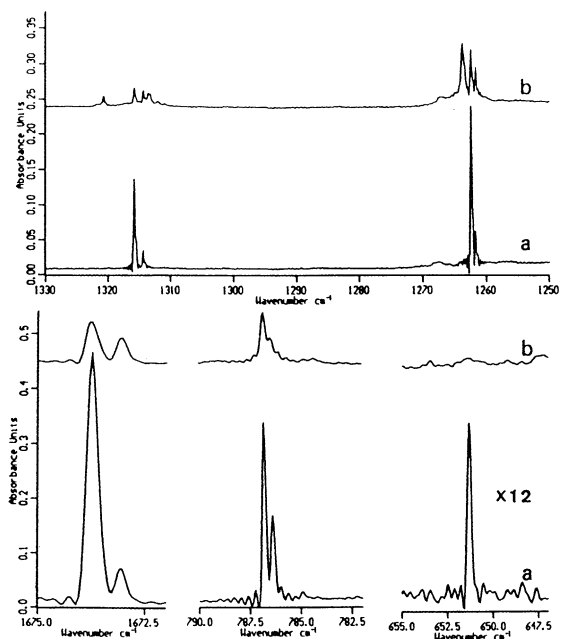


Fig. 1. Infrared spectra of  $\text{ClNO}_2/\text{Ar}$  matrix sample (1/5000) at 10 K: (a) after deposition at 20 K; (b) after annealing at 38 K.

Table 1

Vibrational wavenumbers ( $\text{cm}^{-1}$ ) for IR band positions of  $\text{ClNO}_2$  in the gas phase and trapped in argon, nitrogen and oxygen matrices and their assignment

Modes	Argon matrix	Oxygen matrix	Nitrogen matrix	Gas phase [9]
$\nu_4 = \nu_{\text{AS}}^{\text{NO}} (\text{B}_1)$	1673.8 (1)	1674.4 (1)	1673.1 (1)	1684.6
$\nu_1 = \nu_{\text{S}}^{\text{NO}} (\text{A}_1)$	1261.7 (0.5)	1265.0 (0.65)	1270.5 (0.95)	1267.1
$2\nu_6$	1315.7	1316.2	1324.8	1318.6
<i>Fermi resonance</i>				
$\nu_2 = \delta_{\text{s}} (\text{A}_1)$	786.9 ( $^{35}\text{Cl}$ ) (0.9) 786.4 ( $^{37}\text{Cl}$ )	787.5 (0.7) 787.0	797.3 (0.7) 796.5	792.6 –
$\nu_6 (\text{B}_2)$	651.5 (0.06)	650.8 (0.04)	656.3(0.03)	652.3
$\nu_5 = \delta_{\text{AS}} (\text{B}_1)$	–	–	–	408.1
$\nu_3 = \nu_{\text{S}}^{\text{ClN}} (\text{A}_1)$	–	–	–	369.6

In all matrices the symmetric bending mode  $\nu_2$  of  $\text{A}_1$  symmetry appears as a doublet measured in solid argon at 786.9 and 786.4  $\text{cm}^{-1}$ . The intensity ratio of the two components is 1/3 suggesting that  $\nu_2$  is coupled with  $\nu_3$  (stretching  $\text{N}^{35}\text{Cl}$  and  $\text{N}^{37}\text{Cl}$ ) of the same symmetry. As it can be seen in Fig. 1 the harmonic  $2\nu_6$  band is intense because of Fermi resonance with the  $\nu_1$  mode. Attempts to evaluate the unperturbed frequencies  $\omega_i$  and the Fermi coupling coefficient  $W$  were performed from the observed perturbed frequencies  $\lambda_i$  and the integrated intensity ratio between mixed modes using the simplified following expression established from time independent perturbation theory:

$$\lambda_1 + \lambda_2 = \omega_1 + \omega_2,$$

$$\lambda_1 \lambda_2 = \omega_1 \omega_2 - W^2,$$

$$\frac{I_2}{I_1} = \frac{(\lambda_1 - \lambda_2) - (\omega_1 - \omega_2)}{(\lambda_1 - \lambda_2) + (\omega_1 - \omega_2)}.$$

In argon matrix  $\omega_1$  ( $2\nu_6$ ) and  $\omega_2$  ( $\nu_1$ ) were found to be 1292.6 and 1284.9  $\text{cm}^{-1}$ , respectively, with a Fermi coefficient of 26.75  $\text{cm}^{-1}$ .

Some weak satellite bands were observed near  $\nu_4$  (1673.05  $\text{cm}^{-1}$ ),  $2\nu_6$  (1314.3  $\text{cm}^{-1}$ ),  $\nu_1$  (1261.7  $\text{cm}^{-1}$ ) fundamentals. After annealing at 38 K their relative intensities in regard to the monomer band increased indicating that they belong to dimer species. Other bands which appear after annealing in the  $\nu_4$  region (1313.6–1313.3, 1263.9  $\text{cm}^{-1}$ ) are probably due to higher aggregates than dimers.

## 4. Photo-dissociation of $\text{ClNO}_2$

### 4.1. Observations

$\text{ClNO}_2$  highly diluted in argon matrix (1/5000) was irradiated with the 266 nm laser line. FTIR spectra were recorded after each of several successive irradiation periods. Fig. 2 shows typical spectra obtained after irradiation with a photo-flux of  $9 \times 10^{16}$  photons  $\text{cm}^{-2} \text{s}^{-1}$ . Irradiation caused a decrease in intensity for all bands belonging to  $\text{ClNO}_2$  and new bands appeared at 1754.9, 1710.5, 852–850.7, 658.0 and 640.0  $\text{cm}^{-1}$ . However, as illustrated in Fig. 2, after 20 min of irradiation time, all peaks belonging to  $\text{ClNO}_2$  and those belonging to the photolysis products showed a nearly stationary intensity suggesting a photo-stationary state between  $\text{ClNO}_2$  and the photo-products.

From ab initio calculations [11,12], and experimental data [4,6,7] the band at 1754.9  $\text{cm}^{-1}$ , the doublet at 852–850.7  $\text{cm}^{-1}$  and the feature at 640.0  $\text{cm}^{-1}$  are assigned to  $\nu_{\text{NO}}$ ,  $\delta_{\text{ONO}}$  and  $\nu_{\text{ClO}}$  modes of the *trans*  $\text{ClONO}$  molecule, respectively. Absorptions at 1710.5 and at 640.0  $\text{cm}^{-1}$  are assigned to the  $\nu_{\text{NO}}$  and  $\nu_{\text{ClO}}$  modes of the *cis*  $\text{ClONO}$  molecule, respectively. All observed band positions and the proposed assignment are collected in Table 2 for comparison with the calculated literature data. Thus, under irradiation,  $\text{ClNO}_2$  transforms into *cis* and *trans*  $\text{ClONO}$  isomers but a steady-state concentration is reached on approximately 1200 s of irradiation in this

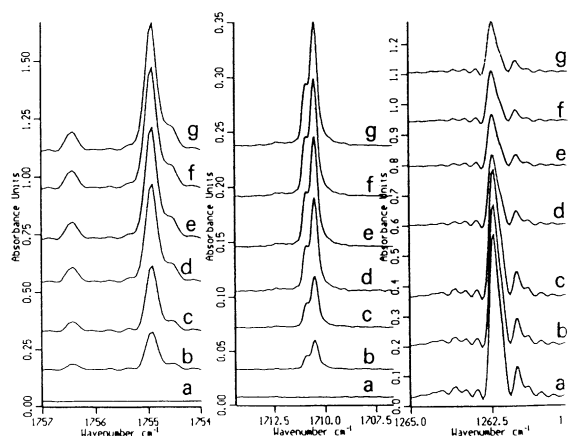


Fig. 2. Product band growth during laser photolysis of  $\text{ClNO}_2/\text{Ar}$  (1/5000) mixture in the  $\nu_{\text{NO}}$  of t-ClONO and c-ClONO. For comparison decrease of  $\text{ClNO}_2$  is shown in the  $\nu_1$  region. Irradiation times in minutes: (a) 0; (b) 120; (c) 240; (d) 600; (e) 1200; (f) 1800 s. Photon flux  $9 \times 10^{16}$  photons  $\text{cm}^{-2} \text{s}^{-1}$ .

experiment. In order to obtain information about the relative stability of the photo-products a subsequent irradiation experiment was carried out with a xenon lamp at  $\lambda > 360$  nm after photolysis of  $\text{ClNO}_2$  at 266 nm and formation of *cis* and *trans* ClONO. As shown in Fig. 3, after 3 h of irradiation time, a decrease in intensity of the  $1754.9 \text{ cm}^{-1}$  absorption was observed with an increase in intensity of the  $1710.5 \text{ cm}^{-1}$  absorption in parallel. Intensity of the  $\text{ClNO}_2$  bands remained unchanged. At  $\lambda > 360$  nm ClONO *trans* transforms partially into ClONO *cis* but total disappearance of ClONO *trans* was not observed with a longer irradiation time, suggesting a reverse isomerization process of *cis* ClONO into *trans* ClO-

NO in the same wavelength range to produce a photochemical equilibrium. As it also can be seen in Fig. 3, in the  $\delta_{\text{ONO}}$  region, the two components of the  $852\text{--}850.7 \text{ cm}^{-1}$  doublet decrease in intensity under irradiation, confirming that they belong to the *trans* ClONO isomer and not, as suggested in [7], to the *trans* and *cis* ClONO isomers, respectively. Assuming that the total population is conserved, i.e., only interconversion and not loss occurs, it is possible to obtain a value of the ratio of the appropriate IR absorption cross-sections of  $\nu_{\text{NO}}$  for the *trans* and *cis* ClONO from measurements of the intensity of the  $\nu_{\text{NO}}$  band of *trans* ClONO which disappears and of the intensity of the  $\nu_{\text{NO}}$  band of *cis* ClONO which appears. The ratio

$$\frac{\varepsilon_{1750}}{\varepsilon_{1715}} = \frac{\varepsilon_t \text{ClONO}}{\varepsilon_c \text{ClONO}}$$

was found equal to  $1.2 \pm 0.2$ , a value in agreement with that determined theoretically by Lee [11].

The knowledge of the ratio  $\varepsilon_t \text{ClONO}/\varepsilon_c \text{ClONO}$  allows one to calculate the relative concentration of *trans* and *cis* ClONO produced at the photo-stationary state after irradiation of  $\text{ClNO}_2$  at 266 nm as well as to obtain molar fractions of each species present in the matrix as a function of the irradiation time at 266 nm using measurements of integrated intensities of  $\text{ClNO}_2$  at time = 0 ( $A_{\text{ClNO}_2}^0$ ) and of  $\text{ClNO}_2$ , c-ClONO and t-ClONO ( $A'$ ) after the different irradiation times ( $t$ ). At each time one should have

$$[\text{ClNO}_2]_0 = [\text{ClNO}_2]_t + [\text{t-ClNO}_2]_t + [\text{c-ClNO}_2]_t$$

and

Table 2

Comparison between frequencies ( $\text{cm}^{-1}$ ) of *cis* and *trans* ClONO observed experimentally in argon matrix and obtained by ab initio calculations from [11]

Modes	CIS		TRANS	
	Argon matrix	ab initio	Argon matrix	ab initio
$\nu_1 = \nu_{\text{NO}} (\text{A}')$	1710.5	1715	1754.9	1754
$\nu_2 = \delta_{\text{ONO}} (\text{A}')$		850	852.0–850.7	855
$\nu_3 = \nu_{\text{ClO}} (\text{A}')$	640.0	638	658.0	662
$\nu_4 = \nu_{\text{ON}} (\text{A}')$		416		407
$\nu_5 = \delta_{\text{ClON}} (\text{A}')$		249		262
$\nu_6 (\text{A}'')$		341		170

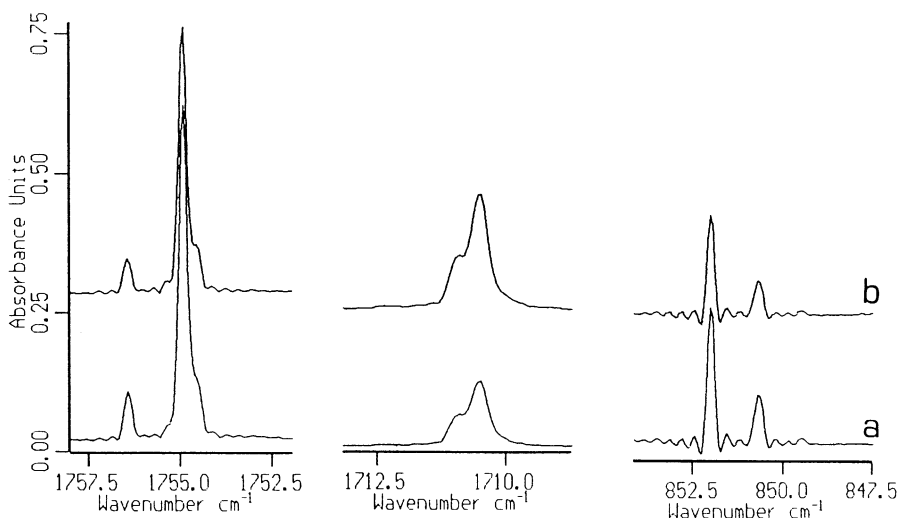


Fig. 3. Effect of irradiation at  $\lambda > 360$  nm during 3 h upon spectra of *t*-CIONO and *c*-CIONO in the 1760–1750, 1715–1700, 860–845  $\text{cm}^{-1}$  regions: (a) spectrum after photolysis at 266 nm of a  $\text{ClNO}_2/\text{Ar}$  (1/5000) mixture; (b) spectrum (a) after photolysis at  $\lambda < 360$  nm.

$$\frac{A_{\text{ClNO}_2}^t}{A_{\text{ClNO}_2}^0} + \frac{A_{t\text{-CIONO}}^t}{A_{\text{ClNO}_2}^0} * a + \frac{A_{c\text{-CIONO}}^t}{A_{\text{ClNO}_2}^0} * b = 1$$

with

$$a = \frac{\epsilon_{\text{ClNO}_2}}{\epsilon_{t\text{-CIONO}}}, \quad b = \frac{\epsilon_{\text{ClNO}_2}}{\epsilon_{c\text{-CIONO}}}, \quad \frac{b}{a} = \frac{\epsilon_{t\text{-CIONO}}}{\epsilon_{c\text{-CIONO}}} = 1.2$$

From experimental measurements of the  $\nu_{\text{NO}}$  intensity for the three compounds,  $a$ , was found to be 0.55. Time evolution of the molar fractions of the various species following irradiation is presented in Fig. 4. At the photo-stationary state 60% of  $\text{ClNO}_2$  is photolysed leading to the formation of 42% of *trans* CIONO and of 18% of *cis* CIONO.

#### 4.2. Photolytic process

Photolysis of  $\text{ClNO}_2$  in the gas phase leads to the formation of Cl and  $\text{NO}_2$ . In matrices the photo-dissociation of  $\text{ClNO}_2$  at 266 nm proceeds probably along the same channel as in gas phase but due to the cage effect, recombination of Cl and  $\text{NO}_2$  in the matrix cage occurs and leads to  $\text{ClNO}_2$  or to *cis* and *trans* CIONO isomers which transform back in  $\text{ClNO}_2$  through Cl and  $\text{NO}_2$  photo-fragments probably without interconversion at this wavelength as follows:

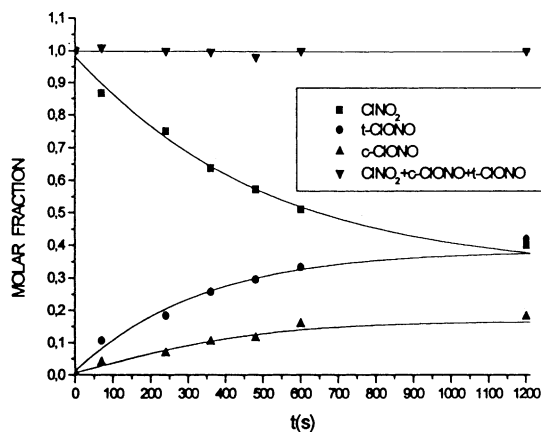
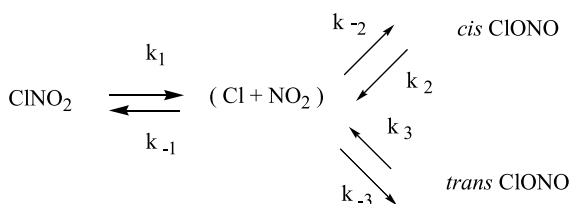


Fig. 4. Curves of the molar fractions of  $\text{ClNO}_2$ , *c*-CIONO, *t*-CIONO species versus photolysis time.

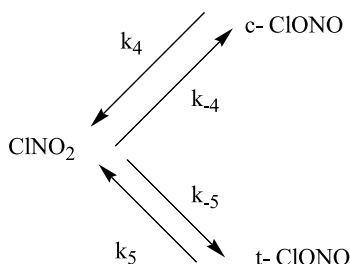


If we assume a stationary state for the  $(\text{Cl} + \text{NO}_2)$  pair, the disappearance rate of  $\text{ClNO}_2$  at each time can be written as

$$\begin{aligned}
 & -\frac{d[\text{ClNO}_2]}{dt} \\
 & = \left(k_1 - \frac{k_1 k_{-1}}{k}\right)[\text{ClNO}_2] - \left(\frac{k_{-1} k_2}{k}\right)[\text{c-ClONO}] \\
 & \quad - \left(\frac{k_{-1} k_3}{k}\right)[\text{t-ClONO}] \quad (1)
 \end{aligned}$$

with  $k = k_{-1} + k_2 + k_{-3}$ .

This equation is similar to that which is obtained with a model simplified as follows:



Indeed from this model

$$\begin{aligned}
 -\frac{d[\text{ClNO}_2]}{dt} & = (k_{-4} + k_{-5})[\text{ClNO}_2] - k_4[\text{c-ClONO}] \\
 & \quad - k_5[\text{t-ClONO}] \quad (2)
 \end{aligned}$$

a differential equation equivalent to (1) supposing

$$(k_{-4} + k_{-5}) = k_1 - \frac{k_1 k_{-1}}{k}, \quad k_4 = \frac{k_{-1} k_2}{k},$$

$$k_5 = \frac{k_{-1} k_3}{k}$$

Furthermore

$$\frac{d[\text{c-ClONO}]}{dt} = k_{-4}[\text{ClNO}_2] - k_4[\text{c-ClONO}] \quad (3)$$

$$\frac{d[\text{t-ClONO}]}{dt} = k_{-5}[\text{ClNO}_2] - k_5[\text{t-ClONO}] \quad (4)$$

At the beginning of the reaction (*i*) concentrations of *cis* and *trans* ClONO are very weak and from (3) and (4)

$$\frac{[\text{t-ClONO}]_i}{[\text{c-ClONO}]_i} = \frac{k_{-5}}{k_{-4}} \quad (5)$$

At the equilibrium state (eq)

$$\begin{aligned}
 -\frac{d[\text{ClNO}_2]_{\text{eq}}}{dt} & = \frac{d[\text{c-ClONO}]_{\text{eq}}}{dt} \\
 & = \frac{d[\text{t-ClONO}]_{\text{eq}}}{dt} = 0 \quad (6)
 \end{aligned}$$

and from (3) and (4)

$$\frac{[\text{t-ClONO}]_{\text{eq}}}{[\text{c-ClONO}]_{\text{eq}}} = \frac{k_4 k_{-5}}{k_{-4} k_5}$$

From kinetic curves of Fig. 3 it can be seen that the ratio  $[\text{t-ClONO}]_i/[\text{c-ClONO}]_i$  is nearly similar to  $[\text{t-ClONO}]_{\text{eq}}/[\text{c-ClONO}]_{\text{eq}}$ . Consequently  $k_4 = k_5$  and Eq. (2) can be written as

$$\begin{aligned}
 -\frac{d[\text{ClNO}_2]}{dt} & = (k_{-4} + k_{-5})[\text{ClNO}_2] \\
 & \quad - k_4([\text{c-ClONO}] + [\text{t-ClONO}]) \quad (7)
 \end{aligned}$$

As  $[\text{c-ClONO}] + [\text{t-ClONO}] = [\text{ClNO}_2]^0 - [\text{ClNO}_2]_t$ , ( $[\text{ClNO}_2]^0$  initial concentration of  $[\text{ClNO}_2]$  at  $t=0$ ), Eq. (7) becomes

$$\begin{aligned}
 -\frac{d[\text{ClNO}_2]}{dt} & = (k_4 + k_{-4} + k_{-5})[\text{ClNO}_2] \\
 & \quad - k_4[\text{ClNO}_2]^0 \\
 & = k'[\text{ClNO}_2] - k_4[\text{ClNO}_2]^0 \quad (8)
 \end{aligned}$$

Finally integration of Eq. (8) gives the concentration of  $\text{ClNO}_2$  at time  $t$ :

$$[\text{ClNO}_2] = [\text{ClNO}_2]^0 \frac{k' \exp^{-k't} - k_4 \exp^{-k_4 t} + k_4}{k'} \quad (9)$$

As the  $[\text{ClNO}_2]$  concentration is proportional to the integrated absorption intensity of  $\text{ClNO}_2$  vibrational modes the experimental decrease in intensity of the  $\nu_{\text{NO}}$  band of  $\text{ClNO}_2$  versus irradiation time was fitted from the kinetic equation (9) using the program Excel Microsoft<sup>®</sup>. The fitting was satisfactory with appropriate coefficients  $k'$  and  $k_4$  which were found from our experimental conditions to be  $2.36 \times 10^{-3}$  and  $8.32 \times 10^{-4} \text{ s}^{-1}$ , respectively. Relative concentrations obtained for *trans* and *cis* ClONO from  $\text{Cl} + \text{NO}_2$  recombination (42% and 18%, respectively) could suggest that the *trans* ClONO is more stable than the *cis* ClONO an observation in disagreement with heats of formation of *cis* ClONO and *trans* ClONO which were predicted to be  $15.4 \pm 1.5$  and  $18.0 \pm$

1.5 kcal mol<sup>-1</sup>, respectively, from ab initio calculations using isodesmic reactions involving H<sub>2</sub>O, HOCl and *cis* HONO and *trans* HONO [11]. In fact due to steric effects recombination of Cl and NO<sub>2</sub> in the matrix cage favours the formation of *trans* ClONO in regard to that of *cis* ClONO.

## 5. Other photolysis channels

The equilibrium state between ClONO<sub>2</sub>, *c*-ClONO and *t*-ClONO observed after irradiation at 266 nm of ClONO<sub>2</sub> is the indication that just as ClONO<sub>2</sub>, ClONO photo-dissociates into Cl and NO<sub>2</sub>. However on prolonged photolysis ( $t > 2500$  s in the above experiment) bands characteristic of the three products decreased slowly in intensity and two new bands located at 1842 and 1804 cm<sup>-1</sup> grew as illustrated in Fig. 5. From their previous identification in this laboratory [13], the two bands at 1842 and 1804 cm<sup>-1</sup> can be assigned to the stretching  $\nu_{NO}$  mode of ClON and ClNO, respectively. Appearance of ClON is the indication that the photo-dissociation of ClONO occurs through a second pathway namely ClON + O.

The formation in parallel of ClNO could also suggest a second dissociation channel for ClONO<sub>2</sub>, but this assumption is very questionable because it has been evidenced that ClON transforms fastly into ClNO in argon matrix by the tunnelling effect [13]. Thus the origin of ClNO is probably due to isomerization of ClON into ClNO. As a matter of fact, the dissociation process ClONO<sub>2</sub> → ClNO + O has a reaction enthalpy equal to 288 kJ mol<sup>-1</sup> and at 248 nm, this decay path was found to be a minor channel ( $\Phi = 0.02$ ) in the gas phase [14].

In order to verify the formation of an oxygen atom as photofragment of ClONO photo-dissociation and to determine its energy state (O<sup>3</sup>P or O<sup>1</sup>D), photolysis of ClONO<sub>2</sub> trapped in two reactive matrices, solid oxygen and nitrogen, was carried out at 266 nm. In oxygen matrices ground state atomic oxygen and excited atomic oxygen which is quickly quenched can react with oxygen host molecules and produce ozone. In nitrogen, excited atomic oxygen O<sup>1</sup>D can react with N<sub>2</sub> molecules leading to N<sub>2</sub>O molecule production.

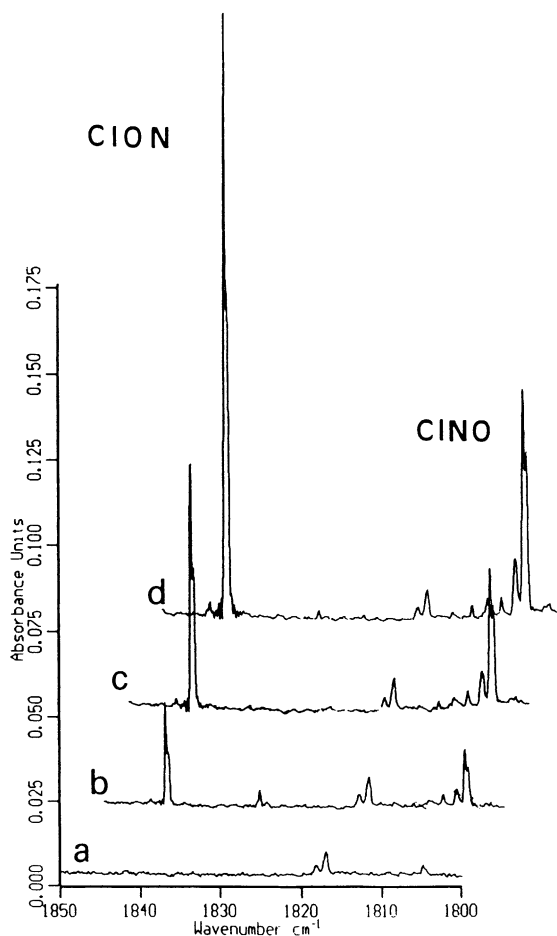


Fig. 5. Product band growth in the 1850–1800 cm<sup>-1</sup> region during prolonged photolysis at 266 nm of the sample of Fig. 2 (ClONO<sub>2</sub>/Ar = 1/5000). Irradiation times: (a) 1800; (b) 3000; (c) 4800; (d) 16200 s.

### 5.1. Oxygen matrix

Oxygen matrix containing 1/5000 of ClONO<sub>2</sub> was subjected to 266 nm photolysis for up to 120 min. Product absorption regions of special interest before photolysis and after different irradiation times are shown in Fig. 6. A higher loss of ClONO<sub>2</sub> than in argon was observed. It was accompanied by the appearance of features associated with *cis* ClONO (1709.5–1708.3 cm<sup>-1</sup>), *trans* ClONO (1754.6–1751.9 cm<sup>-1</sup>), O<sub>3</sub> (2108.2, 1037.9, 702.7 cm<sup>-1</sup>), O<sub>3</sub> ··· O (2096.1, 1030.8, 697.8 cm<sup>-1</sup>) ClNO (1804.6, 1803.7, 1802.7 cm<sup>-1</sup>) and ClONO<sub>2</sub>

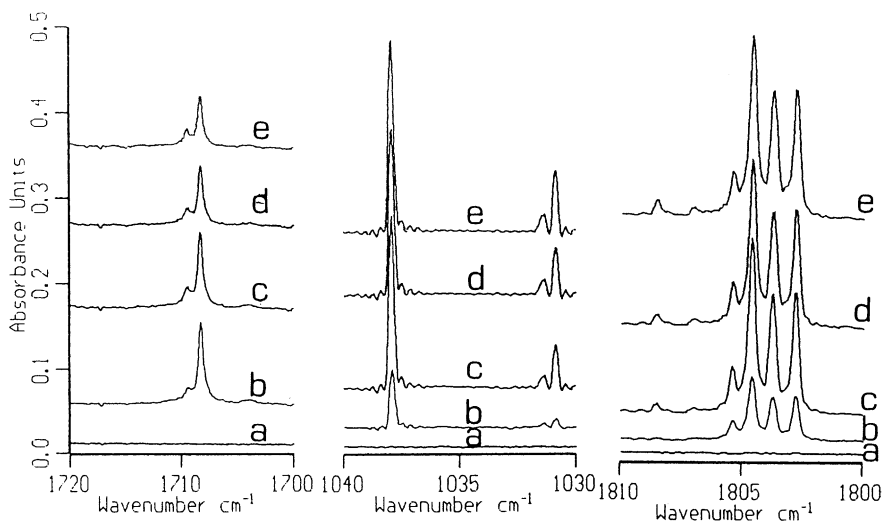


Fig. 6. Product band growth during laser photolysis of a  $\text{ClNO}_2/\text{O}_2$  (1/5000) mixture in typical spectral regions with photolysis times of (a) 5; (b) 30; (c) 60; (d) 120 min.

Table 3

Wavenumbers of infrared absorptions due to products formed on photolysis of Ar,  $\text{O}_2$ ,  $\text{N}_2$  matrices containing  $\text{ClNO}_2$  and their assignment

Argon matrix	Oxygen matrix	Nitrogen matrix	Assignment
		2235.5–2233.4	$\text{N}_2\text{O}$
	2108.2		$\text{O}_3$ ( $\nu_1 + \nu_3$ )
	2096.1		$\text{O}_3 \cdots \text{O}$ ( $\nu_1 + \nu_3$ )
		1881.8–1874.8	$\text{NO}$ , $\text{NO} \cdots \text{X}$
1842		1832–1830–1829	$\text{ClONO}$
		1826.1	asym- $\text{N}_2\text{O}_4$ (D')
1804	1804.6–1803.7–1802.7	1825.5	asym- $\text{N}_2\text{O}_3$
		1823.3–1819	$\text{ClNO}$
		1757.0	asym- $\text{N}_2\text{O}_4$ (D)
1754.9	1754.6–1751.9	1763.1	sym- $\text{N}_2\text{O}_4$
		1759	t- $\text{ClONO}$
	1730.1–1728.9–1721.7		sym- $\text{N}_2\text{O}_3$
1710.5	1709.5–1708.3	1723.5	$\text{ClONO}_2$
		1716.7–1714.8	c- $\text{ClONO}$
		1691.3	sym- $\text{N}_2\text{O}_4$
		1615.9	sym- $\text{N}_2\text{O}_3$
		1295.7–1295.1	$\text{NO}_2$
		1291.3	asym- $\text{N}_2\text{O}_4$ (D)
		1285.2–1282.1	asym- $\text{N}_2\text{O}_4$ (D')
	1037.9		$\text{N}_2\text{O}$
	1030.8		$\text{O}_3$
		853.3	$\text{O}_3 \cdots \text{O}$
852.0–850.7		850.1	sym $\text{N}_2\text{O}_3$
	702.7		t- $\text{ClONO}$
	697.8		$\text{O}_3$
658			$\text{O}_3 \cdots \text{O}$
640			t- $\text{ClON}$
			c- $\text{ClONO}$

(1730.0, 1728.9, 1721.7  $\text{cm}^{-1}$ ) as minor products. The peak locations of product absorptions are listed in column 2 of Table 3. The time dependence of the products is illustrated in Fig. 7. For short photolysis times,  $\text{ClNO}_2$  strongly disappears and as in argon matrix *cis* and *trans* ClONO isomers appear. At longer times, *c*-ClONO and *t*-ClONO decrease at the same rate whatever ClNO grows with a maximum in concentration after 60 mn of irradiation. In parallel ozone appears as well as traces of  $\text{ClONO}_2$  after an induction period. The ClONO isomer was not observed probably due to its rapid conversion into ClNO. Appearance of ozone and its complex with atomic oxygen both identified in the  $\nu_3$  region by absorptions at 1037.9 and at 1030.8  $\text{cm}^{-1}$ , respectively [15] confirm the photo-dissociation of ClONO into ClNO and atomic oxygen. There is no net destruction of ozone because when photo-dissociation of  $\text{O}_3$  occurs the oxygen atom produced combines with oxygen molecule host and regenerates ozone [16].

Only one secondary product, chlorine nitrate, is observed as traces. It is probably produced from the photolysis of ClNO diluted in solid oxygen as reported by Tevault and Smardzewski [17]. Dissociation of  $\text{ClONO}_2$ , which is very slow, can also

occur leading to ClNO and an oxygen atom [18]. However, the induction period observed for  $\text{ClONO}_2$  which is produced in small amounts is the indication that this possible dissociation is a minor channel for the production of ozone observed in this experiment.

## 5.2. Nitrogen matrix

Exposure of  $\text{ClNO}_2/\text{N}_2$  sample (1/5000) to 266 nm irradiation over 8 h produced a product spectrum richer than that observed with argon and oxygen matrices.  $\text{ClNO}_2$  decreased strongly at the beginning of irradiation, and was totally destroyed after 8 h of irradiation. Three new pattern absorptions appeared in the 2250–2000, 1880–1800, 1760–1700, 1300–1250  $\text{cm}^{-1}$  regions with, in addition, absorptions at 1691, 1616, 853 and 852  $\text{cm}^{-1}$ . Fig. 8 shows excerpts of some spectra recorded after different irradiation times and Fig. 9 displays changes in the intensities of main product bands as a function of irradiation times. Table 2 of column 3 lists the IR frequencies of absorptions observed after irradiation. Identification of the numerous close bands was not straightforward principally in the 1800 and 1700  $\text{cm}^{-1}$  regions which is characteristic of products containing  $(\text{NO})_x$  oscillators. Different trapping sites, complexes and aggregates of produced species cannot be excluded. Nevertheless on the basis of their different time evolutions during photolysis correlated to the literature data, the main products were identified.

Bands at 1763, 853 and at 1723.5  $\text{cm}^{-1}$  which showed the same time evolution than in oxygen matrix were assigned to *t*-ClONO and to *c*-ClONO, respectively. The bulky structure centred at 2235  $\text{cm}^{-1}$  which was correlated to two weaker bands at 1282 and 1280  $\text{cm}^{-1}$  was assigned to  $\text{N}_2\text{O}$  in comparison with data reported in the literature [19,20]. Absorption at 1825  $\text{cm}^{-1}$  which grew in concert with  $\text{N}_2\text{O}$  was assigned to the NO stretch ( $\nu_1$ ) mode of ClNO molecule in spite of a red 5  $\text{cm}^{-1}$  shift with respect to the frequency of directly deposited ClNO in nitrogen [13]. As previously evidenced, species produced from photolysis of a site containing the reactant can exhibit a weak shift from directly deposited species. Other

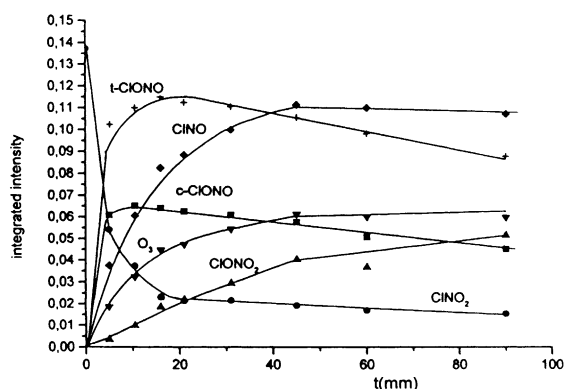


Fig. 7. Time evolution of photoproducts and  $\text{ClNO}_2$  after photolysis at 11 K of a  $\text{ClNO}_2/\text{O}_2$  (1/5000) mixture with the 266 nm laser line using integrated intensities of an absorption of each product. ClNO: pattern bands between 1805.9 and 1802.0  $\text{cm}^{-1}$ ; *t*-ClONO: 1754.6, 1751.9  $\text{cm}^{-1}$ ; *c*-ClONO: 1709.5, 1708.3  $\text{cm}^{-1}$ ;  $\text{O}_3$ : 1037.9  $\text{cm}^{-1}$ ;  $\text{ClNO}_2$ : 1315.6  $\text{cm}^{-1}$ ;  $\text{ClONO}_2$ : pattern absorptions between 1732 and 1718  $\text{cm}^{-1}$ . Integrated intensities of absorption belonging at ClNO and (*c*) and (*t*) ClONO have been reduced by 50%.

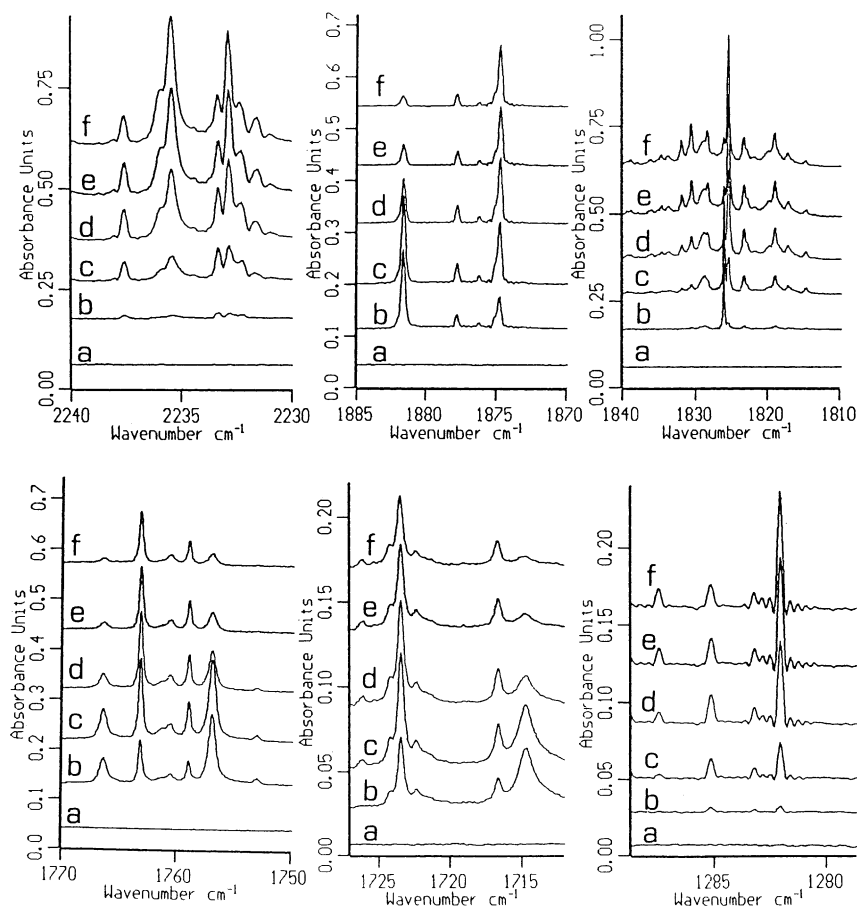


Fig. 8. Product band growth during laser photolysis of a  $\text{ClNO}_2/\text{N}_2$  (1/5000) mixture in typical spectral regions with photolysis times of (a) 0; (b) 15; (c) 60; (d) 190; (e) 370; (f) 500 min.

remaining bands were assigned to NO ( $1881.6\text{ cm}^{-1}$ ),  $\text{NO}\cdots\text{X}$  ( $1874.8\text{ cm}^{-1}$ ),  $\text{NO}_2$  ( $1616\text{ cm}^{-1}$ ) from the literature data [21,22] and to  $\text{N}_2\text{O}_3$  and  $\text{N}_2\text{O}_4$  species as discussed below. Two isomeric forms of  $\text{N}_2\text{O}_3$  (symmetric ONONO and asymmetric ON– $\text{NO}_2$ ) and of  $\text{N}_2\text{O}_4$  ( $\text{O}_2\text{N–NO}_2$  of  $D_{2h}$ , and  $D_{2d}$  symmetries and asymmetric ONO– $\text{NO}_2$ ) have been spectroscopically identified several years ago in gas phase [22], solid phase [22–25] and matrices [26–31]. Varetto and Pimentel [29] showed that in nitrogen matrix asym- $\text{N}_2\text{O}_3$  was converted into sym- $\text{N}_2\text{O}_3$  upon prolonged exposure to the radiation of the Nernst glower source of the infrared spectrometer. On this basis the band at  $1826\text{ cm}^{-1}$  and the absorptions at  $1759$ ,  $1691$  and  $853.3\text{ cm}^{-1}$  were assigned to asym- $\text{N}_2\text{O}_3$  and sym-

$\text{N}_2\text{O}_3$ , respectively. Indeed when the sample was kept in the dark (12 h) after photolysis at  $266\text{ nm}$ , the absorption at  $1826\text{ cm}^{-1}$  disappeared whatever the absorptions at  $1759$ ,  $1691$  and  $853.3\text{ cm}^{-1}$  grew. Observed frequencies for sym- $\text{N}_2\text{O}_3$  are in good agreement with the literature data. Unfortunately, the remaining observed absorptions attributable to asym- $\text{N}_2\text{O}_3$  were overlapped by the  $\text{ClNO}_2$  bands. As shown in Fig. 9(b), asym- $\text{N}_2\text{O}_3$  grows strongly at the beginning of the irradiation then disappears. Consistent with published data, the triplet at  $1832.04$ – $1830.7$ – $1829.0$  and the doublet at  $1823$ – $1819\text{ cm}^{-1}$  with features at  $1291$ – $1295\text{ cm}^{-1}$  were assigned to asym- $\text{N}_2\text{O}_4$  (D and D') and features at  $1757$  and  $1714.8\text{ cm}^{-1}$  to sym- $\text{N}_2\text{O}_4$ . As illustrated in Fig. 9(b), sym- $\text{N}_2\text{O}_4$  at

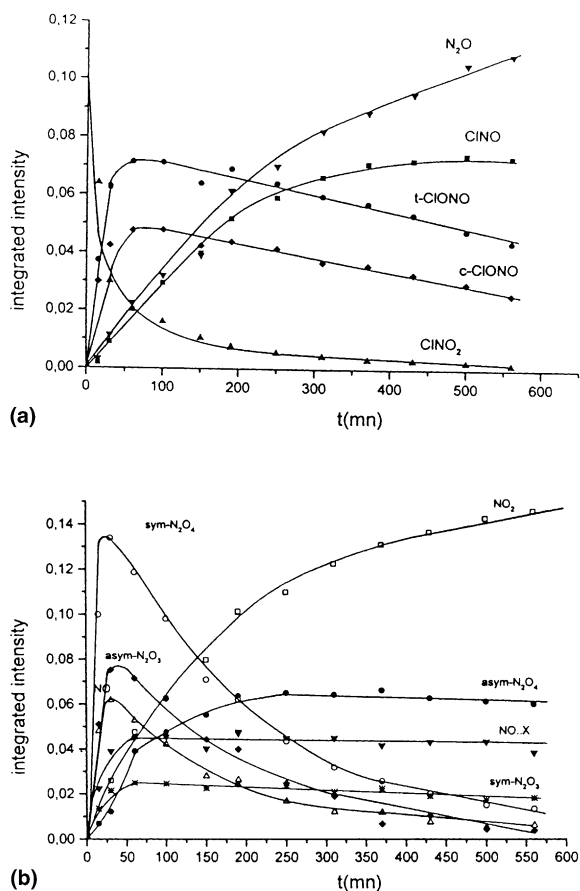


Fig. 9. Time evolution of photoproducts and ClNO<sub>2</sub> after photolysis at 11 K of a ClNO<sub>2</sub>/N<sub>2</sub> (1/5000) mixture with the 266 nm laser line using integrated intensities of an absorption of each product. N<sub>2</sub>O: 2235.5 cm<sup>-1</sup>; ClNO: 1825.5 cm<sup>-1</sup>; t-ClONO: 1763.1 cm<sup>-1</sup>; c-ClONO: 1723.5 cm<sup>-1</sup>; ClNO<sub>2</sub>: 1324.8 cm<sup>-1</sup>; NO<sub>2</sub>: 1615.9 cm<sup>-1</sup>; NO: 1881.8 cm<sup>-1</sup>; NO...X: 1874.8 cm<sup>-1</sup>; asym-N<sub>2</sub>O<sub>3</sub>: 1826.1 cm<sup>-1</sup>; sym-N<sub>2</sub>O<sub>3</sub>: 1759.0 cm<sup>-1</sup>; sym-N<sub>2</sub>O<sub>4</sub>: 1757.0 cm<sup>-1</sup>; sym-N<sub>2</sub>O<sub>4</sub>: 1757.0 cm<sup>-1</sup>; asym-N<sub>2</sub>O<sub>4</sub>: 1830–1827 cm<sup>-1</sup>. Integrated intensities of NO<sub>2</sub>, ClNO<sub>2</sub>, N<sub>2</sub>O have been reduced by 50%, and integrated intensities of ClNO by 33%.

266 nm is sensitive to irradiation and transforms partially into asym-N<sub>2</sub>O<sub>4</sub>. Note that in argon matrix isomerization of asym-N<sub>2</sub>O<sub>4</sub> into sym-N<sub>2</sub>O<sub>4</sub> was observed at 436 nm irradiation as reported by Bandow et al. [32].

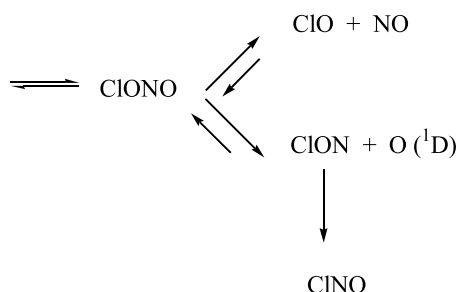
As in argon and oxygen matrix, photo-dissociation of ClNO<sub>2</sub> leads to ClONO which in turns dissociates into ClON and oxygen atom. Formation of N<sub>2</sub>O is the indication that produced oxygen atom is in an excited state. As in oxygen matrix,

ClON is not observed, due to its fast conversion into ClNO which grows in concert with N<sub>2</sub>O. Formation of nitrogen oxides not observed in argon and oxygen matrix is the indication of a third dissociation channel of ClONO. In regard to argon matrix, nitrogen matrix favours the diffusion of small molecules [30,31] and hence cage recombination of photo-fragments can be partially ruled out. Formation of N<sub>2</sub>O<sub>3</sub>, NO and NO<sub>2</sub> at the beginning of irradiation with ClONO suggests that ClONO dissociates also into NO + ClO. In nitrogen matrices the NO molecule cannot result from the decomposition of ClNO as previously observed [13] and hence it is formed from ClONO and leads to N<sub>2</sub>O<sub>3</sub> for which the only known bimolecular channel through which N<sub>2</sub>O<sub>3</sub> can be produced is via the reaction NO<sub>2</sub> + NO → N<sub>2</sub>O<sub>3</sub> [20–26]. Appearance of NO<sub>2</sub> after total destruction of ClNO<sub>2</sub> can be due to photo-dissociation of ClONO or subsequent photolysis of N<sub>2</sub>O<sub>3</sub>, or of sym-N<sub>2</sub>O<sub>4</sub>, or to reaction of NO produced by ClONO with atomic oxygen. Further speculation on this point must await other investigations with isotopically substituted ClNO<sub>2</sub> which are underway.

## 6. Conclusion

Photolysis of ClNO<sub>2</sub> in solid argon at 266 nm as shown by FTIR leads to the formation of *cis* and *trans* ClONO in equilibrium with ClNO<sub>2</sub>. These results indicate that photolysis of ClNO<sub>2</sub> yields Cl + NO<sub>2</sub> that may recombine in the matrix cage to reform ClNO<sub>2</sub> or to produce ClONO which transforms back in Cl + NO<sub>2</sub> fragments. At λ > 360 nm transformation of *trans* ClONO into *cis* ClONO leading to a photochemical equilibrium occurs. The calculated ratio of absorption cross-sections of ν<sub>NO</sub> band for the *trans* and *cis* ClONO shows that the *trans* ClONO is formed in a slightly higher yield than the *cis* ClONO (t-ClONO/c-ClONO = 2.3).

Prolonged photolysis of ClNO<sub>2</sub> at 266 nm in argon, nitrogen, oxygen matrices gives evidence that photo-dissociation of ClONO proceeds along two other different channels namely ClON + O(<sup>1</sup>D) and ClO + NO. Thus photolysis of ClNO<sub>2</sub> at 266 nm can be summarized as follows:



### Acknowledgements

This work was partly supported by PNCA (Programme national de Chimie Atmosphérique) funding.

### References

- [1] W. Behnke, C. George, V. Scheer, C. Zetzsch, *J. Geophys. Res.* 102 (1997) 3795.
- [2] F. Schweitzer, P. Mirabel, C. George, *J. Phys. Chem. A* 102 (1998) 3942.
- [3] K. Drdla, R.P. Turco, S. Elliot, *J. Geophys. Res.* 98 (1993) 8965.
- [4] H. Niki, P.D. Maker, C.M. Savage, L.P. Breitenbach, *Chem. Phys. Lett.* 59 (1978) 78.
- [5] Y. Kawashima, H. Takeo, C. Matsumura, *Chem. Phys. Lett.* 63 (1979) 119.
- [6] D.E. Tevault, R.R. Smardzewski, *J. Chem. Phys.* 67 (1977) 3777.
- [7] D. Scheffler, H. Grothe, H. Willner, A. Frenzel, C. Zetzsch, *Inorg. Chem.* 36 (1997) 335.
- [8] V.M. Schmeisser, *Z. Anorg. Chem.* 256 (1948) 33.
- [9] D.L. Bernitt, R.H. Miller, I.C. Hisatsune, *Spectrochim. Acta A* 23 (1967) 237.
- [10] J. Orphals, M. Morillon-Chapey, G. Guelachvili, *J. Mol. Spectrosc.* 165 (1994) 315.
- [11] T.J. Lee, *J. Phys. Chem.* 98 (1994) 111.
- [12] S.C. Bhatia, J.H. Hall, *J. Chem. Phys.* 82 (1985) 1991.
- [13] A. Hallou, L. Schriver-Mazzuoli, C. Camy-Peyret, A. Schriver, P. Chaquin, *Chem. Phys.* 237 (1998) 251.
- [14] H.H. Nelson, H.S. Johnston, *J. Phys. Chem.* 85 (1981) 3891.
- [15] L. Schriver-Mazzuoli, A. de Saxce, C. Lugez, C. Camy-Peyret, A. Schriver, *J. Chem. Phys.* 102 (1995) 690.
- [16] M. Bahou, L. Schriver-Mazzuoli, A. Schriver, P. Chaquin, *Chem. Phys. Lett.* 173 (1997) 31.
- [17] D.E. Tevault, R.R. Smardzewski, *J. Phys. Chem.* 82 (1978) 375.
- [18] A. de Saxce, L. Schriver-Mazzuoli, *Chem. Phys. Lett.* 199 (1992) 596.
- [19] I. Suzuki, *J. Mol. Spectrosc.* 32 (1969) 5473.
- [20] M. Bahou, L. Schriver-Mazzuoli, C. Camy-Peyret, A. Schriver, T. Chiavassa, J.P. Aycard, *Chem. Phys. Lett.* 265 (1997) 145.
- [21] A. Hinz, J.S. Wells, A.G. Maki, *J. Mol. Spectrosc.* 119 (1998) 120.
- [22] J. Laane, J.R. Ohlsen, *Prog. Inorg. Chem.* 27 (1980) 476.
- [23] C.H. Bibart, G.E. Ewing, *J. Chem. Phys.* 61 (1974) 1293.
- [24] W.G. Fateley, H.A. Bent, B. Crawford, *J. Chem. Phys.* 31 (1958) 204.
- [25] I.C. Hisatsune, J.P. Devlin, Y. Wada, *J. Chem. Phys.* 33 (1960) 714.
- [26] V.R. Morris, S.C. Bahtia, J.H. Hall Jr., *J. Phys. Chem.* 91 (1987) 3359.
- [27] G.R. Smith, W. Guillory, *J. Mol. Spectrosc.* 68 (1977) 223.
- [28] F. Bolduan, H.J. Jodl, *Chem. Phys. Lett.* 85 (1981) 283.
- [29] E.L. Varetti, G.C. Pimentel, *J. Chem. Phys.* 55 (1971) 3813.
- [30] S.C. Bathia, J.H. Hall Jr., *J. Phys. Chem.* 84 (1980) 3255.
- [31] A. Striling, I. Papai, J. Mink, D.R. Salahu, *J. Chem. Phys.* 100 (1994) 2910.
- [32] H. Bandow, H. Akimoto, S. Akiyama, T. Tezuka, *Chem. Phys. Lett.* 111 (1984) 496.